

Car Drag Coefficient Prediction from 3D Point Clouds Using a Slice-Based Surrogate Model

Utkarsh Singh¹[0009-0003-6327-8392], Absaar Ali¹[0009-0004-1408-6690], and Adarsh Roy²[0009-0009-4966-0660]

¹ Delhi Technological University, Shahbad Daulatpur, Delhi, 110042, India

{utkarshsingh_me21b16_52,absaarali_co20b2_24}@dtu.ac.in

² Indian Institute of Technology, Hauz Khas, Delhi, 110016, India

adarsh.roy@iitdalumni.com

Abstract. The automotive industry’s pursuit of enhanced fuel economy and performance necessitates efficient aerodynamic design. However, traditional evaluation methods such as computational fluid dynamics (CFD) and wind tunnel testing are resource intensive, hindering rapid iteration in the early design stages. Machine learning-based surrogate models offer a promising alternative, yet many existing approaches suffer from high computational complexity, limited interpretability, or insufficient accuracy for detailed geometric inputs. This paper introduces a novel lightweight surrogate model for the prediction of the aerodynamic drag coefficient (C_d) based on a sequential slice-wise processing of the geometry of the 3D vehicle. Inspired by medical imaging, 3D point clouds of vehicles are decomposed into an ordered sequence of 2D cross-sectional slices along the stream-wise axis. Each slice is encoded by a lightweight PointNet2D module, and the sequence of slice embeddings is processed by a bidirectional LSTM to capture longitudinal geometric evolution. The model, trained and evaluated on the DrivAerNet++ dataset, achieves a high coefficient of determination ($R^2 > 0.9528$) and a low mean absolute error ($MAE \approx 6.046 \times 10^{-3}$) in C_d prediction. With an inference time of approximately 0.025 seconds per sample on a consumer-grade GPU, our approach provides fast, accurate, and interpretable aerodynamic feedback, facilitating more agile and informed automotive design exploration.

Keywords: Drag Coefficient Prediction · Automotive Aerodynamics · Surrogate Modeling · Slice-Based Model · Point Clouds · Deep Learning

1 Introduction

Aerodynamic efficiency is paramount in the automotive industry, directly impacting fuel economy, emissions, vehicle stability, and the range of electric vehicles. Reducing aerodynamic drag, quantified by the drag coefficient (C_d), is a primary design goal. However, conventional evaluation methods, namely Computational Fluid Dynamics (CFD) and wind tunnel testing, present significant bottlenecks. CFD simulations, while detailed, are computationally expensive and

time consuming, with typical runs taking hours to days and requiring substantial high-performance computing (HPC) resources [6,16]. Wind tunnel tests, though crucial for validation, involve costly facility operation and lengthy model fabrication times [7], limiting their use in the early iterative design phases. These constraints are a hindrance to rapid exploration of the design space.

To overcome these limitations, few machine learning surrogate models have emerged as a promising alternative for rapid aerodynamic prediction [1]. These models learn a complex mapping from vehicle geometry to aerodynamic properties from data generated by high-fidelity simulations. Once trained, they can predict C_d in seconds or milliseconds. However, existing ML surrogates face several challenges. Voxel-based methods, using 3D Convolutional Neural Networks (CNNs), suffer from resolution bottlenecks and can lose fine geometric details [10]. Projection-based methods, which convert 3D shapes into 2D images for 2D CNNs [14], can suffer from information loss due to occlusions or choice of viewpoints and may lack physical interpretability. Point cloud-based methods, such as PointNet [12] and its variants [2,13], operate directly on 3D surface points but often treat points permutation-invariantly, potentially missing crucial directional cues inherent in aerodynamic flow. More recent graph neural networks [4] and transformer-based architectures [8,9,15], while powerful, can be computationally intensive and complex. For instance, TripNet [2] uses triplane representations and achieves high accuracy, but still involves sophisticated geometric processing. Many of these models, particularly complex deep learning architectures, act as "black boxes," offering limited insight into how specific geometric features influence aerodynamic performance.

This paper proposes a novel lightweight, sequential and interpretable approach for C_d prediction. Our core idea is to represent the 3D vehicle geometry as an **ordered** sequence of 2D cross-sectional slices along the primary (streamwise) direction of airflow, analogous to how MRI or CT scans represent 3D anatomical structures. This structured representation explicitly captures the front-to-rear evolution of the vehicle's shape, which is fundamental to its aerodynamic behavior. Each 2D slice, represented as a set of points, is processed by our lightweight **PointNet2D** module (our 2D adaptation of PointNet [12]) to extract local geometric features. The sequence of these per-slice feature embeddings is then fed into a **Bidirectional Long Short-Term Memory (LSTM)** network, which models the dependencies and progression of shape features along the vehicle's length. Finally, a Multi-Layer Perceptron (MLP) regresses the C_d from the LSTM's aggregated representation. This approach offers several advantages :

- **Efficiency:** By processing 2D slices, it avoids the high computational cost of full 3D convolutions or global attention mechanisms on large point clouds.
- **Interpretability:** The model directly captures the flow-aware, front-to-rear progression of the vehicle's shape. This intuitive approach provides a basis for attributing drag contributions to specific longitudinal sections of the vehicle.

We validate our model using the large-scale DrivAerNet++ dataset [5], which provides high-fidelity CFD-computed C_d values for thousands of parametric car

models. Our initial results demonstrate competitive accuracy with state-of-the-art methods, but with significantly reduced computational complexity and enhanced interpretability.

The remainder of this paper is organized as follows: Section 2 details the dataset, data pre-processing techniques, and, the proposed model architecture. Section 3 presents the experimental results, including performance comparisons and training dynamics. Section 4 discusses the implications of these results, limitations, and comparisons. Finally, Section 5 concludes the paper and outlines future research directions.

2 Methods

This section details the dataset, pre-processing steps, the architecture of our proposed slice-based sequential model, and the training procedure.

2.1 Dataset

We utilize the DrivAerNet++ dataset [5], a large-scale multi-modal car aerodynamics dataset. It contains over 8,000 parametric car models, spanning various body styles (fastback, notchback, estateback, SUV) and configurations (e.g., with/without detailed underbodies, rotating wheels). For each model, the dataset provides a 3D mesh, a point cloud representation, and the ground truth drag coefficient (C_d) computed using Reynolds-Averaged Navier-Stokes (RANS) $k-\omega$ SST CFD simulations. We use the point cloud representation provided via the PaddleScience platform [11]. After filtering for complete data, our working dataset comprises 7,713 unique car geometries. We adopt the following split: 5398 samples for training, 1115 for validation, and 1200 for testing. This choice ensures a fair comparison with prior studies, which also evaluated on a 1200-sample test set. The point clouds are consistently oriented with the X-axis along the streamwise direction, Y-axis laterally, and Z-axis vertically.

2.2 Data Pre-processing

The core of our pre-processing pipeline is the conversion of each 3D car point cloud into an ordered sequence of 2D cross-sectional slices.

Cross-Sectional Slicing Each 3D point cloud (typically \sim 100,000 points) is sliced along the primary flow direction (X -axis).

1. **Number of Slices (S):** We chose $S = 80$ slices. This value was empirically found to provide a good balance between capturing sufficient geometric detail along the car’s length and maintaining a manageable sequence length for the LSTM. Too few slices would blur important local features, while too many would increase computational cost and redundancy.

2. **Binning:** For each car, the range of x coordinates (x_{min}, x_{max}) is determined. This range is then divided into S equal bins. The width of each bin w is $(x_{max} - x_{min})/S$.
3. **Projection to YZ-Plane:** All points within the i -th bin (that is, $x \in [x_{min} + (i-1)w, x_{min} + iw)$) are projected onto the YZ-plane by discarding their x coordinate. This results in a set of 2D representing the cross-sectional profile of the car at that longitudinal station.

This process yields a sequence of $S = 80$ slices, each represented by a variable number of 2D points (y, z) . The overall slicing strategy is conceptually depicted in Figure 1, while Figure 2 visualizes the sequence for a sample vehicle, showcasing the detailed evolution of its cross-sectional shape from front to rear.

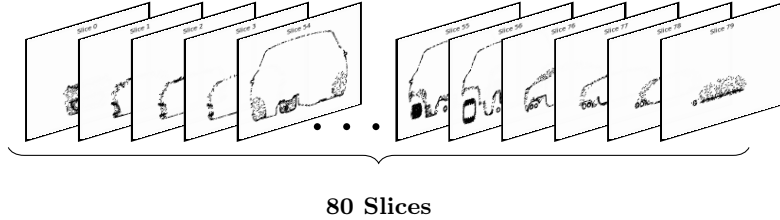


Fig. 1: Illustration of 80 streamwise (x-axis) slices extracted from a car's point cloud. This isometric side view demonstrates how dense slicing captures detailed shape variation from front to back.

Padding and Masking The number of points in each 2D slice varies. To create fixed-size tensors for batch processing, we pad each slice.

- We determined the maximum number of points observed in any single slice in the entire dataset, M_{max} (found to be 6,500).
- Each 2D slice is zero-padded to have M_{max} points. Thus, each slice becomes a tensor of shape $(M_{max}, 2)$.
- A binary mask tensor of shape (S, M_{max}) is created to identify real points and ignore padded entries. Although the mask is available, PointNet2D's global max-pooling is generally robust to zero-padded points, provided features are non-negative.

The final input representation for each car is a tensor of shape $(S, M_{max}, 2)$, i.e., $(80, 6500, 2)$.

2.3 Model Architecture

Our proposed model consists of three main components: a slice-level feature extractor (PointNet2D), a sequence model (Bi-LSTM), and a regression head (MLP). The complete model architecture is depicted in Figure 3.

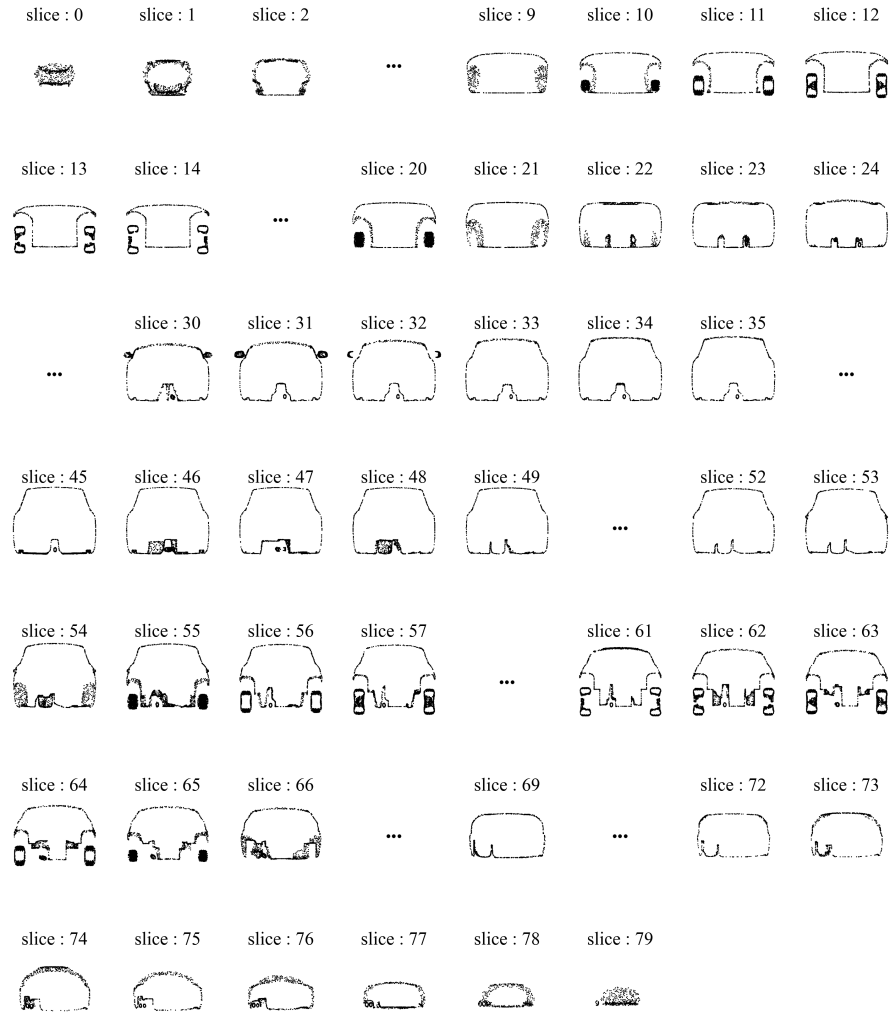


Fig. 2: Visualization of 80 streamwise (X-axis) cross-sectional slices extracted from a vehicle's point cloud. This grid displays the individual 2D point sets, sequentially arranged to highlight the progression of the vehicle's contour from front to back, as used for feature extraction.

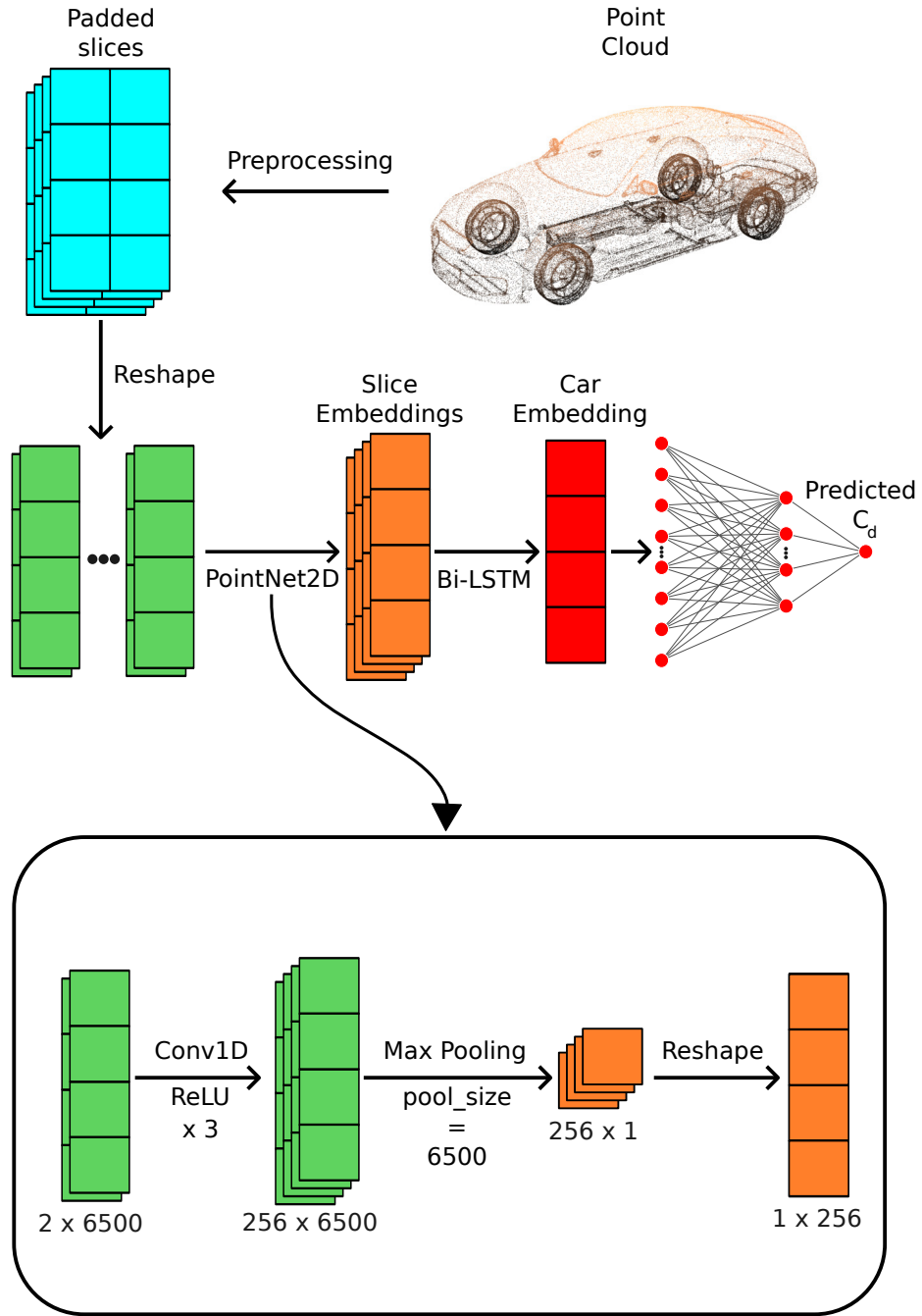


Fig. 3: Complete model architecture of the proposed sequential slice-based drag prediction model. 3D point clouds are sliced. Each slice is encoded by PointNet2D. The sequence of embeddings is processed by a Bi-LSTM and an MLP regresses C_d .

Slice-Level Feature Extraction: PointNet2D Each 2D slice (a set of M_{max} points in \mathbb{R}^2) is processed independently by our PointNet2D module. This module is a simplified adaptation of the original PointNet [12] tailored for 2D point sets and designed to be lightweight. As shown in Figure 3, the PointNet2D module consists of a series of shared 1D convolutional layers (effectively acting as MLPs applied to each point) followed by a global max-pooling operation.

- Input: A slice of shape $(M_{max}, 2)$.
- Layers: Three 1D convolutional layers with kernel size 1. Channel sizes are $2 \rightarrow 32 \rightarrow 64 \rightarrow d_e = 256$. Each convolution is followed by a ReLU activation function.
- Max-Pooling: A global max-pooling operation is applied across the M_{max} points dimension to obtain a single feature vector of dimension $d_e = 256$ for each slice. This ensures permutation invariance for points within a slice.

The output for each car, after this stage, is a sequence of 80 embeddings, resulting in a tensor of shape $(80, 256)$.

Sequence Modeling: Bi-Directional LSTM The sequence of $S = 80$ slice embeddings (each of dimension $d_e = 256$) is processed by a Bidirectional Long Short-Term Memory (Bi-LSTM) network. The Bi-LSTM captures dependencies and contextual information from both forward (front-to-rear) and backward (rear-to-front) directions of the slice sequence.

- Layers: 2 Bi-LSTM layers.
- Hidden Dimension: Each LSTM direction has a hidden state dimension of 256.
- Output: The final hidden states from the forward and backward passes of the last Bi-LSTM layer are concatenated to form a single feature vector representing the entire vehicle. For a hidden dimension of $h=256$, this process creates a 512-dimensional car-level embedding.

Regression Head: MLP The 512-dimensional car embedding from the Bi-LSTM is fed into a Multi-Layer Perceptron (MLP) to regress the scalar C_d value.

- Layers: The MLP consists of three fully connected layers: $512 \rightarrow 256 \rightarrow 64 \rightarrow 1$.
- Activations: ReLU activations are used after the first two layers. A dropout layer with a rate of 0.3 is applied after the first ReLU for regularization.
- Output: A single scalar value representing the predicted C_d .

The total number of trainable parameters in the model is approximately 2.79 million. A summary of the model’s component-wise structure, derived directly from its PyTorch implementation, is as follows:

```

CdPredictor(
  (pointnet): PointNet2D(
    (slice_encoder): Sequential(
      (0): Conv1d(2, 32, kernel_size=(1,), stride=(1,))
      (1): ReLU(inplace=True)
      (2): Conv1d(32, 64, kernel_size=(1,), stride=(1,))
      (3): ReLU(inplace=True)
      (4): Conv1d(64, 256, kernel_size=(1,), stride=(1,))
      (5): ReLU(inplace=True)
    )
  )
  (sequential_encoder): LSTMSliceEncoder(
    (lstm): LSTM(256, 256, num_layers=2, batch_first=True,
                 dropout=0.2, bidirectional=True)
  )
  (regressor): CdRegressor(
    (net): Sequential(
      (0): Linear(in_features=512, out_features=256, bias=True)
      (1): ReLU()
      (2): Dropout(p=0.3, inplace=False)
      (3): Linear(in_features=256, out_features=64, bias=True)
      (4): ReLU()
      (5): Linear(in_features=64, out_features=1, bias=True)
    )
  )
)

```

2.4 Training Details

- **Loss Function:** We use the Smooth L1 Loss (Huber Loss), as defined in Equation 1, which is less sensitive to outliers than Mean Squared Error and provides smooth gradients.

$$\mathcal{L}(y, \hat{y}) = \begin{cases} 0.5(y - \hat{y})^2, & \text{if } |y - \hat{y}| < \beta \\ \beta(|y - \hat{y}| - 0.5\beta), & \text{otherwise} \end{cases} \quad (1)$$

We use $\beta = 1.0$.

- **Optimizer:** Adam optimizer with an initial learning rate of 1×10^{-4} .
- **Batch Size:** A batch size of 4 was used due to GPU memory constraints with the large M_{max} .
- **Epochs:** The model was trained for 100 epochs, and the best model was selected based on the highest R^2 score on the validation set.
- **Hardware:** A single NVIDIA RTX 4060 Laptop GPU.

3 Results

This section presents the performance of our proposed slice-based sequential model. We first define the evaluation metrics, then provide quantitative comparisons with state-of-the-art methods, discuss computational efficiency, and finally analyze training dynamics and error distributions.

3.1 Evaluation Metrics

We use standard regression metrics to evaluate model performance:

- **Mean Squared Error (MSE):** $\frac{1}{N} \sum_{i=1}^N (\hat{y}_i - y_i)^2$.
Measures the average squared difference between predicted and true values.
- **Mean Absolute Error (MAE):** $\frac{1}{N} \sum_{i=1}^N |\hat{y}_i - y_i|$.
Measures the average absolute difference, less sensitive to outliers than MSE.
- **Coefficient of Determination (R^2):** $1 - \frac{\sum_{i=1}^N (\hat{y}_i - y_i)^2}{\sum_{i=1}^N (y_i - \bar{y})^2}$.
Represents the proportion of variance in the dependent variable that is predictable from the independent variables. An R^2 of 1 indicates perfect prediction.
- **Maximum Absolute Error (MaxAE):** $\max_i |\hat{y}_i - y_i|$. Indicates the worst-case prediction error.

For these metrics, y_i is the true C_d , \hat{y}_i is the predicted C_d , \bar{y} is the mean of true C_d values, and N is the number of samples.

3.2 Quantitative Performance

We compare our model’s performance on the DrivAerNet++ test set (1200 samples) against several published surrogate models. Table 1 summarizes these results. Our PointNet2D + BiLSTM model achieves an R^2 of 0.9528 and an MAE of 6.046×10^{-3} .

Table 1: Quantitative comparison of drag-prediction models on the DrivAerNet++ test set.

Model	Dataset subset	MSE (10^{-5})	MAE (10^{-3})	MaxAE (10^{-2})	R^2
PointNet2D+BiLSTM (Ours)	DrivAerNet++ (1200)	6.50	6.046	4.50	0.9528
TripNet [2]	DrivAerNet++ (1200)	9.10	7.17	7.70	0.957
RegDGCNN [4] ^a	DrivAerNet++ (1200)	14.20	9.31	12.79	0.641
PointNet [12] ^a	DrivAerNet++ (1200)	14.90	9.60	12.45	0.643

^a Reported in [5].

Our model demonstrates performance comparable to the state-of-the-art TripNet on DrivAerNet++ in terms of R^2 , while significantly outperforming earlier methods like RegDGCNN and PointNet. The low MAE indicates that, on average, our predictions are very close to the true C_d values.

3.3 Computational Efficiency

Our model is lightweight, with 2.79 million parameters, and achieves the average inference time of 0.025 seconds per sample on an NVIDIA GeForce RTX 4060 Laptop GPU demonstrating the model's suitability for real-time feedback on consumer-grade hardware.

3.4 Training Dynamics and Error Analysis

The model was trained for 100 epochs in a single, end-to-end process. Figure 4a shows the Smooth L1 training loss curve, indicating steady convergence. Figure 4b displays the validation R^2 score per epoch, with the best performance achieved at epoch 68, which was selected as the final model.

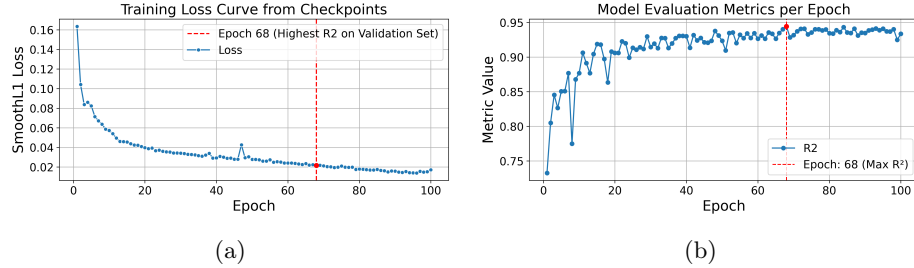


Fig. 4: Training dynamics: (a) Training loss curve. (b) Validation R^2 score over epochs. Best validation R^2 was achieved at epoch 68.

To analyze the prediction quality on the test set, Figure 5 presents a scatter plot of predicted versus true C_d values and a histogram of prediction errors.

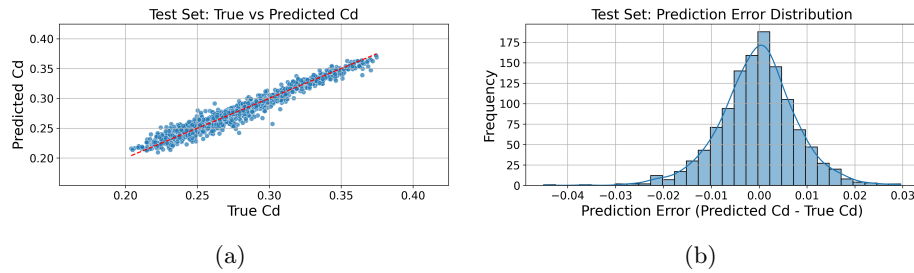


Fig. 5: Test set performance analysis: (a) Scatter plot showing strong correlation between predicted and true C_d values. (b) Histogram of prediction errors, centered near zero with small spread.

The scatter plot (Figure 5a) shows a tight clustering of points around the $y = x$ line, indicating high agreement between the predictions and the ground truth. The error histogram (Figure 5b) is unimodal and centered close to zero, with the majority of errors falling within a narrow range (e.g., $\pm 0.015C_d$). This demonstrates that the model generalizes well to unseen data and does not exhibit significant systemic bias. The MaxAE of 0.045 indicates that even the largest errors are within a reasonable range for early-stage design guidance.

4 Discussion

The results presented in Section 3 demonstrate that our proposed sequential slice-based model achieves high accuracy and efficiency for aerodynamic drag prediction. The R^2 value of 0.9528 on the DrivAerNet++ test set signifies that the model captures over 95% of the variance in drag coefficients, performing comparably to more complex state-of-the-art methods such as TripNet [2], while using a simpler architecture and fewer parameters. The low MAE of approximately 6.046×10^{-3} indicates that the average prediction error is very small, making it a reliable tool for shortlisting design candidates.

The effectiveness of the slice-based approach can be attributed to its ability to explicitly model the geometric evolution of the vehicle’s shape along the **streamwise axis**, a progression that is critical to drag formation. Aerodynamic drag is highly sensitive to how the cross-sectional area and shape change from the front of the vehicle to the rear. By processing an ordered sequence of 2D slices in this direction, the PointNet2D module learns salient features from each local cross-section, and the Bi-LSTM integrates this information to learn the impact of these **progressive changes**. This sequential analysis is key; slicing in other directions, such as at right angles to the flow, would fail to capture this **crucial front-to-back narrative**, as each slice would contain parts of the vehicle’s front, middle, and rear, thereby losing the causal geometric information beneficial for drag prediction. This limitation is also found in methods that treat the point cloud as an unordered set.

A key advantage of our model is its computational efficiency. With an inference time of ~ 0.025 seconds per sample on a consumer-grade GPU, it is substantially faster than traditional CFD and many complex deep learning surrogates (e.g., those based on 3D convolutions or full transformers on point clouds). This speed is critical for early-stage design, enabling engineers to rapidly evaluate numerous design variations, perform sensitivity analyses, and conduct shape optimization interactively. Furthermore, the relatively low parameter count contributes to faster training times and reduced risk of overfitting, especially when datasets might be limited for very specific vehicle types not yet covered by large public benchmarks.

Compared to other approaches, our method strikes a balance between performance and interpretability. While global 3D methods like PointNet or DGCNNs can be powerful, their permutation-invariant nature or complex graph structures can make it difficult to understand which parts of the geometry contribute most

to the prediction. Our slice-based sequence allows, at least conceptually, for an investigation into how individual slices or segments of slices influence the final C_d prediction through analysis of LSTM activations or attention mechanisms if a transformer were used for sequence modeling. This potential for enhanced interpretability, by linking drag to longitudinal sections, can provide designers with more actionable feedback.

Despite its strengths, the proposed method has limitations.

1. **Inter-slice Information Loss:** While 80 slices provide good resolution, some fine 3D geometric details that do not significantly alter the 2D profile of any single slice but exist between slice planes or are inherently 3D in nature (e.g., complex underbody channels, small winglets with specific orientations not aligned with slices) might not be fully captured. The projection onto the YZ plane also means that 3D curvature within a slice's thickness is lost.
2. **Surface-only Scalar Prediction:** The current model predicts only the scalar C_d value and does not provide information about pressure or velocity fields on the vehicle surface or in the surrounding flow. Such field predictions are valuable for detailed aerodynamic analysis and are offered by some more complex surrogate models [2,3].
3. **Absence of Explicit Physics Priors:** The model is purely data-driven. It does not inherently enforce physical laws like conservation of mass or momentum. This could lead to less robust predictions for out-of-distribution shapes not well-represented in the training data.
4. **Fixed Number of Slices:** The choice of $S = 80$ slices was based on empirical observation. An adaptive slicing strategy, allocating more slices to regions with higher geometric variation, could improve performance or efficiency but would also introduce additional complexity.

The broader impact of such a fast and accurate surrogate model is the potential to democratize aerodynamic analysis in the early stages of automotive design. It allows for more extensive design space exploration, leading to potentially more aerodynamically efficient vehicles developed in shorter timeframes and at lower costs.

5 Conclusion

This paper introduced a lightweight and efficient neural network architecture for predicting automotive aerodynamic drag coefficients (C_d) from 3D vehicle point clouds. Our novel approach transforms the 3D geometry into an ordered sequence of 2D cross-sectional slices along the streamwise axis. These slices are individually encoded using a PointNet2D module, and their sequential geometric evolution is captured by a bi-directional LSTM, with a final MLP regressing the C_d .

Trained and evaluated on the large-scale DrivAerNet++ dataset, our model achieved a coefficient of determination (R^2) of 0.9528 and a mean absolute error

(MAE) of 6.046×10^{-3} . These results are competitive with more complex state-of-the-art surrogate models, demonstrating the efficacy of the slice-based sequential representation. A key advantage of our method is its computational efficiency, with an inference time of approximately 0.025 seconds per vehicle on a consumer-grade hardware and a modest parameter count of 2.79 million. This enables rapid aerodynamic feedback, facilitating extensive design iteration and optimization in the early conceptual phases of vehicle development. The inherent structure of the model, focusing on longitudinal geometric progression, also offers potential for enhanced interpretability compared to global "black-box" 3D models.

Future work will focus on several avenues. Enhancing slice encoding with more sophisticated 2D shape descriptors or exploring advanced sequence models like transformers could further improve accuracy. Extending the model to predict surface pressure distributions or even simplified flow fields would provide richer aerodynamic insights. Investigating adaptive slicing techniques and incorporating physics-informed neural network principles could enhance robustness and accuracy, particularly for out-of-distribution geometries. Ultimately, integrating such fast and interpretable surrogate models into interactive CAD tools holds the promise of significantly accelerating and improving aerodynamic design in the automotive industry.

Disclosure of Interests. The authors have no competing interests to declare that are relevant to the content of this article.

References

1. Akasaka, K., Chen, F., Teraguchi, T.: Surrogate model development for prediction of car aerodynamics using machine learning. *Nissan Technical Review* **89**, 79–84 (2022). https://www.nissan-global.com/EN/TECHNICALREVIEW/PDF/NISSAN_TECHNICAL REVIEW_89_En_ALL.pdf, accessed: 2025-09-08
2. Chen, Q., Elrefaie, M., Dai, A., Ahmed, F.: TripNet: Learning large-scale high-fidelity 3D car aerodynamics with triplane networks. *arXiv preprint* (2025). <https://doi.org/10.48550/arXiv.2503.17400>
3. Choy, C., Kamenev, A., Kossaifi, J., et al.: Factorized implicit global convolution for automotive computational fluid dynamics prediction. *arXiv preprint* (2025). <https://doi.org/10.48550/arXiv.2502.04317>
4. Elrefaie, M., Ahmed, F., Dai, A.: Drivaernet: A parametric car dataset for data-driven aerodynamic design and graph-based drag prediction. In: *ASME 2024 International Design Engineering Technical Conferences and Computers and Information in Engineering Conference* (11 2024). <https://doi.org/10.1115/DETC2024-143593>
5. Elrefaie, M., Morar, F., Dai, A., Ahmed, F.: DrivAerNet++: A large-scale multi-modal car dataset with computational fluid dynamics simulations and deep learning benchmarks. In: *Thirty-eighth Conference on Neural Information Processing Systems Datasets and Benchmarks Track* (2024). <https://doi.org/10.48550/arXiv.2406.09624>
6. Ferrari, S., Pipolo, D., Fontanesi, S.: An automated computational fluid dynamics workflow for simulating the internal flow of race car radiators. *Fluids* **8**(7), 202 (2023). <https://doi.org/10.3390/fluids8070202>

7. Ford Motor Company: Ford invests \$200M in new wind tunnel facility. Press Release (2017), https://www.motorauthority.com/news/1108886_ford-invests-200m-in-new-wind-tunnel-facility, accessed: 2025-09-08
8. He, J., Luo, X., Wang, Y.: DrivAer transformer: A high-precision and fast prediction method for vehicle aerodynamic drag coefficient based on the DrivAerNet++ dataset (2025). <https://doi.org/10.48550/arXiv.2504.08217>
9. Jiang, J., Li, G., Jiang, Y., Zhang, L., et al.: TransCFD: A transformer-based decoder for flow field prediction. *Engineering Applications of Artificial Intelligence* **123**, 106340 (2023). <https://doi.org/10.1016/j.engappai.2023.106340>
10. Liu, Z., Tang, H., Lin, Y., Han, S.: Point-voxel CNN for efficient 3D deep learning. In: *Advances in Neural Information Processing Systems*. vol. 32 (2019). <https://doi.org/10.48550/arXiv.1907.03739>
11. PaddleScience Contributors: Drivaernet++ paddlescience documentation (2025), <https://paddlescience-docs.readthedocs.io/zh-cn/latest/zh/examples/drivaernetplusplus/#drivaernet>, accessed: 2025-05-12
12. Qi, C.R., Su, H., Mo, K., Guibas, L.J.: PointNet: Deep learning on point sets for 3D classification and segmentation. In: *Proceedings of the IEEE Conference on Computer Vision and Pattern Recognition (CVPR)*. pp. 652–660 (2017). <https://doi.org/10.1109/CVPR.2017.16>
13. Qi, C.R., Yi, L., Su, H., Guibas, L.J.: PointNet++: Deep hierarchical feature learning on point sets in a metric space. In: *Advances in Neural Information Processing Systems*. vol. 30, pp. 5099–5108 (2017), <https://proceedings.neurips.cc/paper/7095-pointnet-deep-hierarchical-feature-learning-on-point-sets-in-a-metric-space.pdf>
14. Song, J., et al.: Data-driven car drag prediction with depth and normal renderings. *Journal of Mechanical Design* **146**(5), 051714 (2024). <https://doi.org/10.1115/1.4068104>
15. Xiang, H., Ma, Y., Dai, Z., Wang, C., Zhang, B.: AeroDiT: Diffusion transformers for Reynolds-Averaged Navier-Stokes simulations of airfoil flows. *arXiv preprint* (2024). <https://doi.org/10.48550/arXiv.2412.17394>
16. Zacks Equity Research: ANSS sets CFD simulation record using AMD GPUs. Online Article (2025), <https://www.nasdaq.com/articles/anss-sets-cfd-simulation-record-using-amd-gpus-frontier-supercomputer>, accessed: 2025-09-08